

Quantum quincunx in cavity quantum electrodynamics

Barry C. Sanders and Stephen D. Bartlett

*Department of Physics and Centre for Advanced Computing – Algorithms and Cryptography,
Macquarie University, Sydney, New South Wales 2109, Australia*

Ben Tregenna and Peter L. Knight

Optics Section, Blackett Laboratory, Imperial College London, London SW7 2BW, England

(Dated: 4 April 2002)

We introduce the quantum quincunx, which physically demonstrates the quantum walk and is analogous to Galton’s quincunx for demonstrating the random walk. In contradistinction to the theoretical studies of quantum walks over orthogonal lattice states, we introduce quantum walks over *nonorthogonal* lattice states (specifically, coherent states on a circle) to demonstrate that the key features of a quantum walk are observable albeit for strict parameter ranges. A quantum quincunx may be realized with current cavity quantum electrodynamics capabilities, and precise control over decoherence in such experiments allows a remarkable *decrease* in the position noise, or spread, with increasing decoherence.

Galton’s quincunx [1] is a valuable device for demonstrating the random walk (RW): gravity draws pellets through a pyramidal structure of pegs, yielding a binomial distribution. The RW is of fundamental importance as the underlying process for dissipation and fluctuation [2] and as a central concept in research into computer algorithms, which has motivated research into the quantum walk (QW) [3, 4, 5, 6] as a quantum counterpart to the RW. The QW exhibits surprising features such as a quadratic enhancement of fluctuations and possible exponential speedups [7] over the RW. In addition, the QW could be useful for benchmarking the performance of certain quantum devices [8]. Following Galton’s classical example, we describe a cavity quantum electrodynamic (CQED) device that exhibits the QW, with controllable decoherence that can yield a continuous transition from the QW to the RW. Although the (energy-conserving) QW on a circle has been studied [4], and a physical realization in the context of the ion trap has been introduced [8], ideal lattice states have always been assumed; however, orthogonal localized lattice states are not realized physically – typically they would be constructed as nonorthogonal Gaussian (e.g., coherent) states. We prove here that the QW is viable using such nonorthogonal lattice states for a restricted range of energies, still exhibiting the dramatic features characterizing the QW. Moreover, whereas the fluctuation–dissipation theorem yields increased fluctuations as losses increase, this ‘quantum quincunx’ exhibits the counterintuitive result that fluctuations *decrease* as losses increase.

Microwave CQED provides an excellent technology for realizing the quantum quincunx. The combined atom+cavity system can be effectively isolated from the environment, and decoherence can be controllably introduced [9]; furthermore new technologies allow the atom to be struck by a periodic sequence of off-axis microwave pulses [10]. Whereas the RW utilises a random number (a coin toss) to determine right or left steps by the ‘walker’,

the unitary evolution of the QW demands a ‘quantum coin’ that is rotated from the heads (+) or tails (–) state into an equal superposition of these states via the unitary Hadamard transformation [11]. In the CQED realization discussed here, a two-level atom traversing the cavity serves as the quantum coin, and a periodic sequence of $\pi/2$ pulses implement the ‘coin flipping’ Hadamard transformations. Between these Hadamard transformations, the atom interacts with the initially coherent cavity field via a Raman transition to effect a conditional phase shift on the cavity field that depends on the state of the atom. This QW corresponds to the quantum version of the RW on the circle [5]. Whereas both walks exhibit increasing phase fluctuations with time, the QW spreads quadratically faster than the RW.

A potential realization of the QW for the ion trap [8] has a comparable mathematical description, but that analysis implicitly assumes the preparation of harmonic oscillator phase states [12, 13] of ionic motion (analogous to the cavity field state considered here): such states would correspond to lattice states on the circle, but preparation of such states is not feasible. We consider the field initially prepared in a coherent state, achievable with existing technology, and consider the consequences of this initial state.

We begin by introducing the formalism of the QW on the circle embedded in a harmonic oscillator. The discrete QW, corresponding to the RW on the circle, requires a Hilbert space of finite dimension d . For $\{|j\rangle, j < d\}$ the harmonic oscillator number states with fewer than d bosons, we introduce the (finite-dimensional) orthonormal phase state representation [13, 14]

$$|\theta_k = 2\pi k/d\rangle = \frac{1}{\sqrt{d}} \sum_{j=0}^{d-1} \exp(ij\theta_k) |j\rangle, \quad k \in \mathbb{Z}_d, \quad (1)$$

with the Hilbert space for the walker given by $\mathcal{H}_d = \text{span}\{|\theta_k\rangle, k \in \mathbb{Z}_d\}$. For \hat{N} the number operator on \mathcal{H}_d ,

defined by $\hat{N}|j\rangle = j|j\rangle$, the rotation operator $R_l = \exp(i\theta_l \hat{N})$, $l \in \mathbb{Z}_d$ acts on phase states according to $R_l|\theta_k\rangle = |\theta_{k+l}\rangle$. That is, R_l rotates a phase state by an angle θ_l . The operator \hat{N} is the generator of these rotations.

A QW is realized by a sequence of alternating transformations, beginning with a Hadamard transformation of the two-level system (the coin) and followed by a conditional rotation of the state of the walker. The coin is described by a state in a two-dimensional internal Hilbert space \mathcal{H}_2 with basis states $|\pm\rangle$. The Hadamard transformation $\mathbf{H} = \frac{1}{\sqrt{2}}\begin{pmatrix} 1 & 1 \\ 1 & -1 \end{pmatrix}$ acts only on the internal state of the coin (i.e., on \mathcal{H}_2), and transforms a basis state $|\pm\rangle$ into the superposition $\frac{1}{\sqrt{2}}(|+\rangle \pm |-\rangle)$. For $\hat{\sigma}_z = \begin{pmatrix} 1 & 0 \\ 0 & -1 \end{pmatrix}$, the conditional rotation operator

$$\mathbf{F} = \exp\left(\frac{2\pi i}{d} \hat{N} \otimes \hat{\sigma}_z\right) \quad (2)$$

rotates the state of the walker by an angle $\pm 2\pi/d$ conditioned on the coin state $|\pm\rangle$; i.e., $\mathbf{F}(|\theta_k\rangle \otimes |\pm\rangle) = |\theta_{k\pm 1}\rangle \otimes |\pm\rangle$, leaving the coin state unchanged. Thus, beginning with the coin in the $|+\rangle$ state and the walker in the phase state $|\theta_0\rangle$, the evolution is described by repeated, and reversible, application of the unitary operation $\mathbf{U} = \mathbf{F}\mathbf{H}$. Thus, the coin and walker degrees of freedom become entangled. After n iterations, with the coin+walker in the state $|\Psi_n\rangle = \mathbf{U}^n|\theta_0\rangle \otimes |+\rangle$, the probability that the walker is measured at angle θ_k is

$$P_k = |(\langle\theta_k| \otimes \langle + |) |\Psi_n\rangle|^2 + |(\langle\theta_k| \otimes \langle - |) |\Psi_n\rangle|^2. \quad (3)$$

This distribution exhibits the quadratic gain in phase diffusion over the corresponding RW.

We present a scheme to implement a QW on a circle in a microwave cavity, where the spatial state of the walker is represented by the state of a single cavity mode, and the state of the coin is represented by the state of a Rydberg atom passing through the cavity; a diagram of this scheme is presented in Fig. 1. The field mode in the cavity is described by a harmonic oscillator, with an infinite-dimensional Hilbert space \mathcal{H}_{HO} . We wish to use states in this Hilbert space to model a finite-dimensional QW on a circle with discrete lattice points. To do this modelling, we employ a truncated Hilbert space and define the spatial state of the QW to be given by the projection of the cavity mode state onto the subspace \mathcal{H}_d of states with no more than $d-1$ photons. Also, we wish to employ a coherent state as an initial state for the QW, rather than the unphysical phase state $|\theta_0\rangle$. To realize the quantum coin, consider for example a Rydberg atom with two atomic states $\{|+\rangle, |-\rangle\}$.

To implement a QW on a circle, we must implement the Hadamard transformation \mathbf{H} that places the coin in a superposition of the basis states $|\pm\rangle$, and the conditional rotation \mathbf{F} . The Hadamard transformation is realized by a $\pi/2$ pulse on the $|+\rangle \rightarrow |-\rangle$ transition [10]. For an

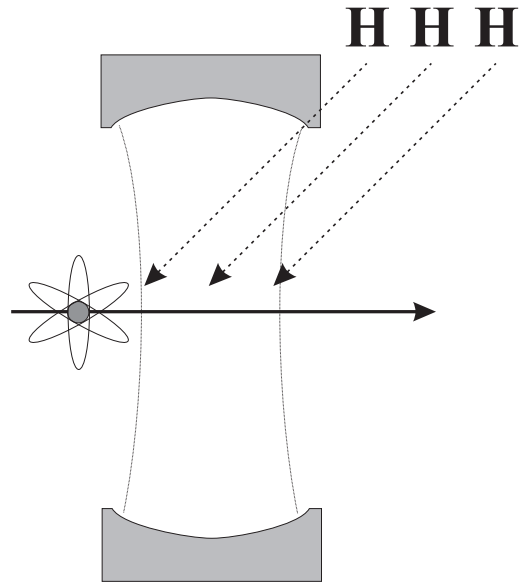


FIG. 1: Schematic for the proposed experiment. A single atom traversing through the cavity is subjected to periodic Hadamard transformations realized as $\pi/2$ pulses. Between these pulses, the cavity field undergoes a phase shift conditioned on the atomic state.

atom initially in the state $|+\rangle$, this $\pi/2$ pulse produces the state $\frac{1}{\sqrt{2}}(|+\rangle + |-\rangle)$. This Hadamard transformation is assumed to act instantaneously and is applied with period τ . To implement the conditional rotation operator \mathbf{F} , we employ the two-level model including ac-Stark shifts [15, 16]. The atomic levels $|+\rangle$ and $|-\rangle$ are highly detuned from the cavity field, and the Hamiltonian for this effect is given by $\hat{H} = \hbar\chi\hat{N} \otimes \hat{\sigma}_z$. This Hamiltonian can be used to generate the conditional rotation operator \mathbf{F} of Eq. (2) on the subspace $\mathcal{H}_d \subset \mathcal{H}_{\text{HO}}$. If the atom+cavity evolve according to this Hamiltonian for time τ between application of the Hadamard transformations, the angle of conditional rotation of the cavity field is given by $\theta = \chi\tau$.

Equivalently, the conditional rotation can be implemented using a three-level system as in the experiment of Rauschenbeutel *et al* [17]. Let $|i\rangle$, $|g\rangle$ and $|e\rangle$ be the states with principal quantum number $n = 49, 50, 51$ respectively. The state $|g\rangle$ represents the internal basis state $|+\rangle$, and the state $|i\rangle$ represents the internal basis state $|-\rangle$. Employing an off-resonant transition between $|g\rangle$ and $|e\rangle$ (with the state $|i\rangle$ uninvolved), the effective Hamiltonian is $\hat{H} = \hbar\chi\hat{N} \otimes |g\rangle\langle g|$. By moving to a rotating description, this Hamiltonian can effect the conditional rotation operator \mathbf{F} . The Hadamard transformation is realized by a $\pi/2$ pulse on the $|g\rangle \rightarrow |i\rangle$ transition.

It is important that the same quantum coin (realized as the Rydberg atom) is used for each step of the QW, because the atomic state becomes entangled with the state of the field. Experimentally, this constraint requires

that the sequence of alternating \mathbf{H} and \mathbf{F} transformations must be implemented during the passage time of a single atom.

The standard initial conditions for the QW would be to have the field (the walker) in the phase state $|\theta_0\rangle$. Constructing a field state that projects to this phase state in \mathcal{H}_d is not feasible. However, it is possible to initiate the cavity in a coherent state $|\alpha\rangle$, with α real and positive, that has a well-defined phase relative to the local oscillator used for homodyne detection. Let $|\alpha\rangle_d$ be the projection of $|\alpha\rangle$ onto \mathcal{H}_d . We require that $|\alpha\rangle_d$ satisfies the overlap condition

$$\langle\theta_j|\alpha\rangle_d \simeq \delta_{j0}, \quad j \in \mathbb{Z}_d. \quad (4)$$

For a given dimension d , the magnitude of α must be chosen such that the coherent state $|\alpha\rangle$ has reasonable support on \mathcal{H}_d . To ensure this support, we employ the condition $d > \bar{n} + \sqrt{\bar{n}}$, where $\bar{n} = |\alpha|^2$ is the mean photon number in the coherent state $|\alpha\rangle$. Also, to satisfy the overlap condition (4), the spacing of the circular lattice must be sufficiently large. Defining the standard quadrature phase space [18] with $\hat{x} = (\hat{a} + \hat{a}^\dagger)/\sqrt{2}$ and $\hat{p} = (\hat{a} - \hat{a}^\dagger)/\sqrt{2}i$, a coherent state has a minimum uncertainty diameter (measured in terms of quadrature standard deviations) of unity. For coherent states with mean photon number of \bar{n} , the circle of radius $\sqrt{\bar{n}}$ can fit approximately $2\pi\sqrt{\bar{n}}$ distinguishable coherent states. Thus, we require that $d < 2\pi\sqrt{\bar{n}}$. Thus the QW can be performed only for a range of possibilities for coherent state amplitudes satisfying $\bar{n} < 28$ and dimension $d < 2\pi\sqrt{\bar{n}}$.

The method of measuring a phase shift of an initial coherent cavity field using a ‘homodyning’ method [17] is proposed here to measure the resulting phase distribution of the cavity field, and thus analyze the QW. Once the atom has left the cavity, a coherent local oscillator field with amplitude α and phase φ relative to the initial field is injected into the cavity, which adds coherently to the cavity field and gives a resulting amplitude in the range 0 to 2α . This technique can be utilized to obtain the probability distribution of the QW as a function of angle for a range of angles near the initial coherent state. Obtaining the phase distribution relies on measuring an ensemble of identical states; it is key to the successful observation of a QW that the conditions of the experiment are identical for each run, and that there is no source of stochasticity that would destroy the quantum interference effects.

We investigate numerically the QW as described above, with $\alpha = 5$ (and thus $\bar{n} = 25$) and $d = 31$. It is assumed that the Hadamard transformation applied to the atomic states occurs effectively instantaneously and is independent of the location of the atom in the cavity. Cavity losses are simulated via an interaction between the single-mode cavity field and an external, low temperature reservoir and are characterized by a loss parameter g . The atom+cavity thus evolves for a time τ between

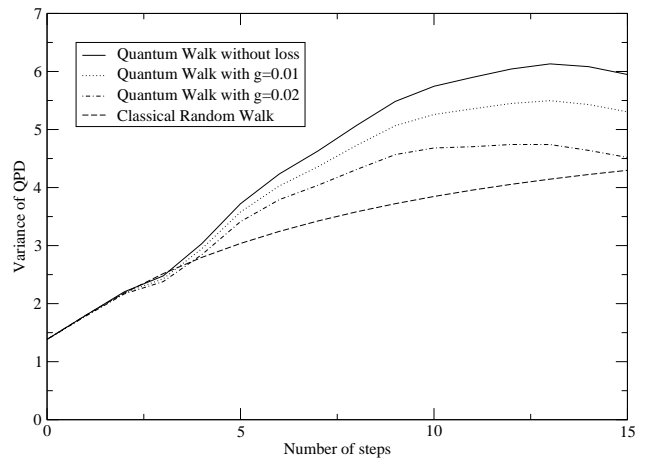


FIG. 2: Plot of the quadrature phase variance as a function of the number of steps for $\alpha = 5$ and $d = 31$.

Hadamard transformations by the master equation

$$\begin{aligned} \frac{d}{dt}\rho(t) = & [\chi a^\dagger a \otimes \sigma_z, \rho(t)] \\ & - \frac{g}{2} (a^\dagger a \rho(t) + \rho(t) a^\dagger a + 2a^\dagger \rho(t) a), \quad (5) \end{aligned}$$

where χ is chosen such that $\chi\tau = 2\pi i/d$. Note that the spatial dependence of χ on the mode structure of the cavity can easily be incorporated into the numerical simulations. A constant step size $\chi\tau$ could still be maintained with such a spatial dependence simply by adjusting the frequency of Hadamard transformations accordingly as the atom traverses the cavity.

We can simulate the outcome of homodyne measurement and thereby obtain the resulting quadrature phase distribution (QPD) on the orthogonal axis to the initial coherent state. The simulated variance of the QPD as a function of the number of steps for a lossless cavity is given in Fig. 2. The variance of the QPD of a classical RW for the same values of α and d obtained by allowing a different atom with a random atomic state to pass through the cavity during each time step is given for comparison. Also shown are the results for the QW in a lossy cavity with loss term $g = 0.01$. Fig. 2 shows clearly the quadratic speed-up in phase diffusion given by the QW over the RW beyond three steps. This plot also reveals the transition from the QW to the RW via increasing cavity loss; thus, the addition of decoherence results in reduced phase fluctuations. Note that the variances for the QW and the RW are identical for the first three steps of the walk (prior to the effects of quantum interference), and that the initial values of these variances are not zero due to the width of the initial coherent state.

The QPD approximates the phase distribution for small θ . Fig. 2 shows that the rate of spreading for the QW is approximately linear from three to ten steps. Beyond ten steps, the rate of spreading decreases as the

QPD deviates from the actual phase distribution. (For the values of α and d used in the simulation, the phase distribution of the QW is localised at $\pm\pi$ after 10 steps.) For this range where the QPD approximates the actual phase distribution, the system clearly exhibits the quadratically-enhanced phase fluctuations expected of a QW.

In conclusion, we have shown that a quantum quincunx, which realizes the QW, can be implemented using existing experimental techniques in a microwave cavity by taking advantage of a physically realistic, nonorthogonal basis of coherent states on a circle in phase space. This quantum quincunx demonstrates the remarkable property that entanglement between the cavity field and a single atom can lead to enhanced phase diffusion over an analogous RW, as well as a controllable transition from the QW to the RW as evidenced by a decrease in the rate of phase diffusion. Decreased phase diffusion resulting from the introduction of decoherence contrasts sharply with intuition from the fluctuation-dissipation theorem: that the introduction of loss (decoherence) yields increased noise. The quantum quincunx is a remarkable tool to demonstrate a QW, which provides quadratic or even exponential speedups over the RW, yields a counterintuitive reduction in phase noise as decoherence increases and opens the way to new explorations of quantum information theory and its experimental implementation.

BCS and SDB acknowledge the support of an Australian Research Council Large Grant and a Macquarie University Research Grant. BT and PLK acknowledge the support of the U. K. Engineering and Physical Sciences Research Council. This project was also funded in part by the European Union project QUIPROCONE (IST-1999-29064). We acknowledge helpful discussions

with S. Haroche, V. Kendon, G. J. Milburn, G. Noguez, B. C. Travaglione and F. Yamaguchi.

-
- [1] F. Galton, *Natural Inheritance* (Macmillan, London, 1889).
 - [2] A. Einstein, *Ann. Phys. (Leipzig)* **17**, 549 (1905).
 - [3] Y. Aharonov *et al*, *Phys. Rev. A* **48**, 1687 (1992).
 - [4] A. Ambainis *et al*, "One-dimensional quantum walks," in *Proceedings of the 33rd Annual ACM Symposium on Theory of Computing* (ACM Press, New York, 2001), p. 37.
 - [5] D. Aharonov *et al*, "Quantum walks on graphs," in *Proceedings of the 33rd Annual ACM Symposium on Theory of Computing* (ACM Press, New York, 2001), p. 50.
 - [6] T. D. Mackay *et al*, *J. Phys. A: Math. Gen.* **35**, 2745 (2002).
 - [7] J. Kempe, [quant-ph/0205083](https://arxiv.org/abs/quant-ph/0205083) (2002).
 - [8] B. C. Travaglione and G. J. Milburn, *Phys. Rev. A* **65**, 032310 (2002).
 - [9] J. M. Raimond *et al*, *Phys. Rev. Lett.* **79**, 1964 (1997).
 - [10] F. Yamaguchi *et al*, *Phys. Rev. A* **66**, 010302(R) (2002).
 - [11] M. A. Nielsen and I. L. Chuang, *Quantum Computation and Quantum Information* (Cambridge University Press, Cambridge, 2000).
 - [12] R. Loudon, *The Quantum Theory of Light* (Clarendon, Oxford, 1973).
 - [13] D. T. Pegg and S. M. Barnett, *J. Mod. Optics* **44**, 225 (1997).
 - [14] V. Bužek *et al*, *Phys. Rev. A* **45**, 8079 (1992).
 - [15] H. Moya-Cessa *et al*, *Opt. Comm.* **85**, 267 (1991).
 - [16] J. M. Raimond *et al*, *Rev. Mod. Phys.* **73**, 565 (2001).
 - [17] A. Rauschenbeutel *et al*, *Phys. Rev. Lett.* **83**, 5166 (1999).
 - [18] R. Loudon and P. L. Knight, *J. Mod. Opt.* **34**, 709 (1987).